Nano Today 25 (2019) 27–37

Contents lists available at ScienceDirect

Nano Today

journal homepage: www.elsevier.com/locate/nanotoday

Review

A review of graphene-based 3D van der Waals hybrids and their energy applications

Hao-Fan Wang, Cheng Tang, Qiang Zhang*

Beijing Key Laboratory of Green Chemical Reaction Engineering and Technology, Department of Chemical Engineering, Tsinghua University, Beijing 100084, China

ARTICLE INFO

Article history:
Received 1 November 2018
Received in revised form 20 January 2019
Accepted 26 February 2019
Available online 7 March 2019

Keywords:
van der Waals hybrids
3D graphene-based nanostructure
Lithium batteries
Electrocatalysis
Energy storage materials

ABSTRACT

Different kinds of 2D materials can be well hybridized by constructing van der Waals heterostructures of them. Among various kinds of 2D materials, graphene has caught the most attention attributed to its superior electronic and mechanical features. To fully maintain and demonstrate their intrinsic features, 3D nanostructured graphene materials are proposed and can be realized by the *in-situ* curving of graphene layers or the post-assembly of graphene nanosheets. Furthermore, by the integration of 3D graphene framework and other 2D materials, graphene-based 3D van der Waals hybrids can be obtained with superior performances and promising applications in various energy fields. In this review, recent advances on graphene-based 3D van der Waals hybrids for energy applications were summarized, highlighting the hybrids between graphene and transition-metal dichalcogenides, other transition metal compounds, metal-free 2D materials, and multiple 2D materials. We hope this review can inspire more innovative insights into this emerging topic in energy materials.

Contents

Introduction

The recent advances in energy research can be boosted by the exploration of emerging building blocks for highly efficient energy materials. Since graphene was firstly isolated in 2004 [1], the family of two-dimensional (2D) materials has been strongly considered worldwide and their applications in energy conversion and storage are also highly concerned. Great efforts have been made on the investigation of graphene-analogous 2D materials, including graphene materials, graphitic carbon nitride (g-C_3N_4), transition-metal dichalcogenide (TMD), layered double hydroxide (LDH), etc., in the fields of energy electrocatalysis [2,3], supercapacitors [4–6], metal-ion batteries [7–10], and so on [11–16]. In addition to the direct employment of an individual 2D material due to its unique properties, the merging of different 2D components to form van der Waals (vdW) heterostructures towards favorable structural and electronic varieties is emerging as a versatile route for materials innovation [17]. The assembly of different 2D material layers is analogous to the building of LEGO blocks, but via the interplanar van der Waals interactions. In fact, the van der Waals interactions are not limited to interplanar interactions in layered materials, but also between any passivated, dangling-bond-free surface [18]. Consequently, various vdW heterostructures can be fabricated through the rational hybridization of different 2D materials, which can

* Corresponding author.
E-mail address: zhang-qiang@mails.tsinghua.edu.cn (Q. Zhang).

https://doi.org/10.1016/j.nantod.2019.02.006
1748-0132/

effectively combine multi-functionalities, compensate individual weakness, and even endow new properties, leading to significantly enhanced performances in energy-related applications [19–23].

Theoretically, graphene is featured with outstanding intrinsic properties as an atomic-thick 2D material, such as high electrical and thermal conductivity, and high mechanical strength. [24–27] However, the graphene products obtained and utilized for energy-related applications are always in the form of powder, which is difficult to fully maintain and demonstrate the intrinsic features [28]. Recently, the concept of three-dimensional (3D) graphene has been proposed and verified [29–31]. By constructing 3D graphene framework with sp^2 configuration, the excellent intrinsic properties of 2D graphene can be inherited into 3D nanostructures [32]. Based on the 3D graphene material instead of its 2D parent, 3D vdW hybrids of other 2D materials supported by 3D graphene can be therefore constructed. The concept of 3D vdW hybrids is an extension of the vdW hybrids of 2D materials, in which 2D materials are likewise hybridized by interplanar vdW interactions, while a 3D structure is formed through curving, stacking, or pore-creating. The integration of 2D and 3D materials is a challenging topic with great significance [33], and 3D vdW hybrids are promising to build a bridge between two- and three-dimensional materials. Benefited by the good electrical conductivity and abundant pore structures of 3D graphene for accelerated electron and mass transfer, the graphene-based 3D vdW hybrids will explore more possibilities of 2D materials, leading to unexpected performances in energy-related applications. Generally, the 3D graphene framework used for constructing graphene-based 3D vdW hybrids is constructed by continuous graphene layers or interconnected graphene nanosheets, exhibiting a 3D hierarchical porous structure. The nanosheets of other 2D materials are in-situ grown or post-deposited on the graphene framework, forming vdW heterostructures. The application performance of the obtained 3D vdW hybrids are mainly determined by the various properties of the additional 2D materials supported by graphene, meanwhile the 3D graphene framework can enhance the electrical conductivity, enlarge the surface area, and make the nanosheets of the 2D material more uniformly dispersed and fully accessible, thus boosting the superb performance in energy-related applications.

Though the concept of 3D vdW hybrids emerges very recently, there were some reported nanocomposites with the configuration of 2D materials combined with 3D graphene before the 3D vdW concept was proposed. For a better understanding of the present advances and new insights for the further development in this field, herein we summarize the graphene-based 3D vdW hybrids, mainly classified into the hybrid between graphene and TMDs, other transition metal compounds, metal-free 2D materials, and multiple 2D materials, together with their energy applications, as illustrated in Fig. 1. The synthetic strategies, unique properties, and electrochemical performances of each family of 3D vdW hybrids are reviewed in details, with some perspectives included. We hope to provide an overview of the recent progress of the emerging graphene-based 3D vdW hybrids, and also expect to inspire more works on the smart design of 2D materials for various energy applications.

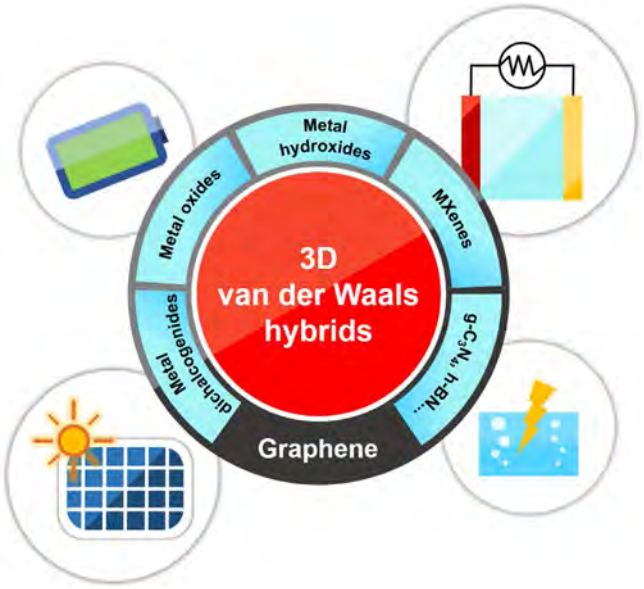

Fig. 1. Schematic of several types of graphene-based 3D vdW hybrids and their energy applications.

3D vdW hybrids of transition metal dichalcogenides and graphene

Transition metal dichalcogenides are an important family of 2D materials, and are widely investigated in the fields of optoelectronics [34], semiconductors [35], electrochemical energy storage [16,36,37], etc. [38]. The dichalcogenides of Mo and W (for instance, MoS_2, $MoSe_2$, WS_2, etc.) are acknowledged for their high reactivity for hydrogen evolution reaction (HER) [39–41]. Therefore, these 2D TMDs are regarded as promising alternatives for Pt-based electrocatalysts in hydrogen-involved energy electrocatalysis. Due to the poor electrical conductivity of TMDs, carbon-based conductive additives are required to bring out their full potential in the electrochemical evaluation [42]. In 3D vdW hybrids of TMDs and graphene, the dichalcogenide layer and the conductive graphene layer are attached to each other in parallel. Thus, the two kinds of 2D materials can be effectively integrated, further facilitating the electron transport and electrochemical reactivities.

The integration of MoS_2 and graphene has always been considered as an efficient way to obtain HER electrocatalysts with superior performance. In 2013, the marriage of MoS_2 and 3D graphene framework in HER electrocatalysis was firstly reported by Liu et al. [43]. Conductive mesoporous graphene foam was synthesized from graphene oxide (GO) via a silica-templated method. Then MoS_2 nanoparticles were deposited on the graphene framework after hydrothermal treating of graphene and $(NH_4)_2MoS_4$. The MoS_2 nanoparticles were highly dispersed in the MoS_2/graphene hybrid, allowing rapid charge transfer at the interface. However, the type of interaction between the two kinds of 2D materials was not clarified in this work. Hereafter, the hybridization of MoS_2 and 3D graphene continues to attract strong attention. A series of metal dichalcogenides/3D graphene hybrid electrocatalysts, including MoS_2 on porous carbon aerogel [43], WS_2 on heteroatom-doped graphene films [44], and MoS_2/$MoSe_2$ on graphene networks [45], were reported.

With the deepening of the understandings on the interfacial contact between 2D materials, the concept of vdW heterostructure was introduced to guide the design of TMDs/3D graphene hybrids and afforded explanations on the performance enhancement of the hybrids. Recently, a 3D vdW hybrid of nitrogen-doped MoS_2 and 3D mesoporous graphene, named G@N-MoS_2, was reported for trifunctional energy electrocatalysis of HER, oxygen reduction reaction (ORR) and oxygen evolution reaction (OER) [46]. The schematic illustration of the nanostructure of G@N-MoS_2 is shown in Fig. 2a. The heterostructure was synthesized through a two-step sequential chemical vapor deposition (CVD) method. Mesoporous 3D graphene was firstly grown on MgO template at a high temperature, following by the deposition of N-MoS_2 at a low temperature. The graphene and N-MoS_2 layers were connected by vdW interaction, as illustrated in Fig. 2a.

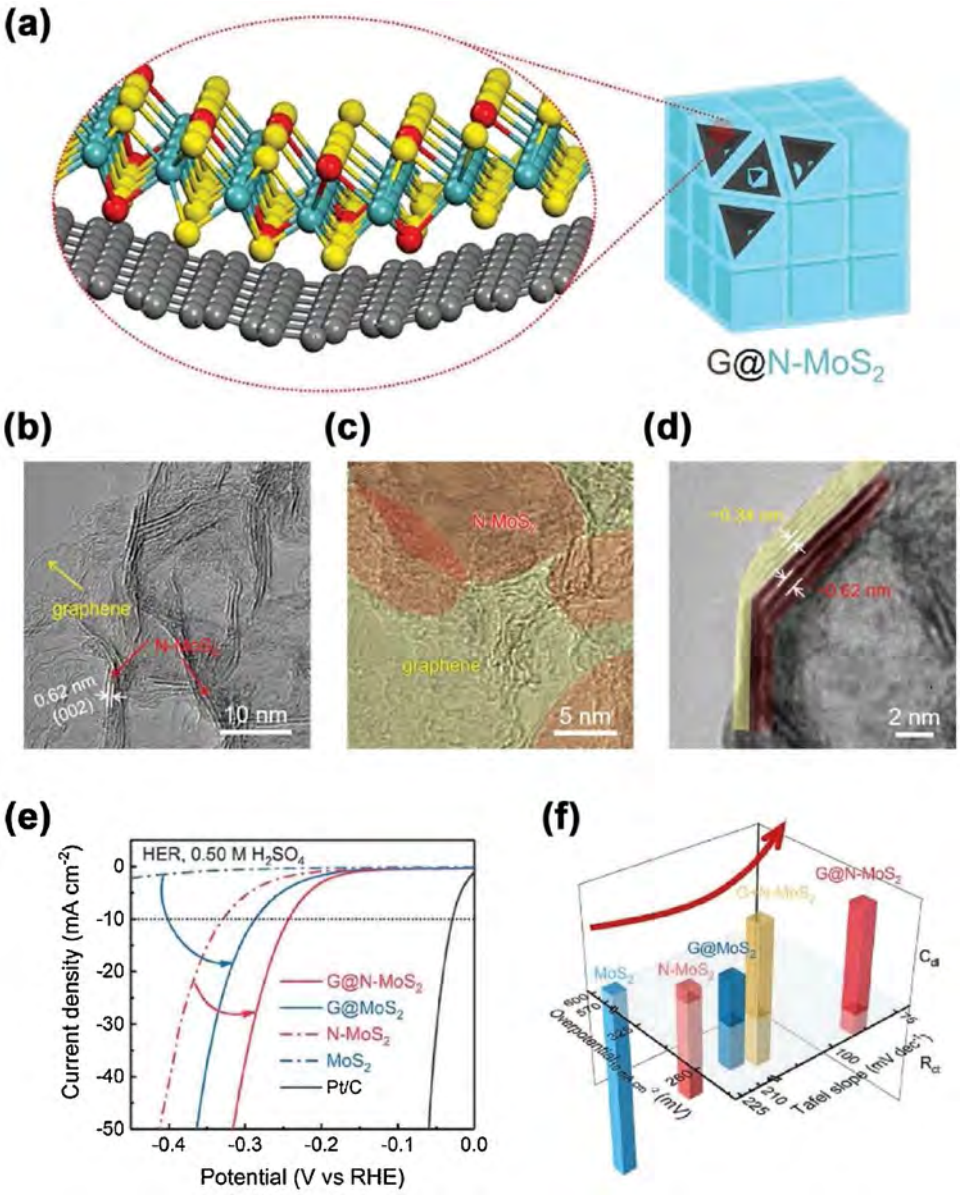

Fig. 2. The hybrid of nitrogen-doped MoS_2 and 3D mesoporous graphene for HER electrocatalysis. (a) The schematic illustration of G@N-MoS_2. (b–d) HRTEM images of G@N-MoS_2. (e) Hydrogen evolution LSV plots tested in 0.50 M H_2SO_4 electrolyte. (f) Summary of overpotentials for 10 mA cm^{-2} HER current density and Tafel plots for the electrocatalysts.

Reproduced with permission from Ref. [46]. Copyright 2018, Wiley-VCH.

The high-resolution transmission electron microscopy (HRTEM) images of G@N-MoS_2 are exhibited in Fig. 2b-d. N-MoS_2 nanosheets (interlayer distance: 0.62 nm) were deposited on the 3D graphene framework. Fig. 2c and 2d provide clear evidence of the layer-by-layer stacking in the vdW hybrids in different directions. N-MoS_2 and graphene, with different interlayer distances, are stacked with the assistance of the vdW force between them. Other characterizations such as electron energy loss spectroscopy (EELS) and X-ray photoelectron spectroscopy (XPS) were also performed to confirm the N doping in MoS_2. Based on the structural characterizations, the 3D mesoporous vdW heterostructure of few-layer graphene and N-MoS_2 was identified, with the advantages of hierarchical pore structure and exquisite integration of 2D materials.

The HER performance of G@N-MoS_2 was evaluated in 0.50 M H_2SO_4 electrolyte. The N-doping and hybridization with 3D graphene bring about significant improvement on the HER activity of G@N-MoS_2 (Fig. 2e). Fig. 2f shows the summary of the overpotential for 10 mA cm^{-2} HER current density, Tafel slope, double layer capacity (C_{dl}, representing the electrochemical active surface area), and charge transfer resistance (Rct, representing the resistance of surface reactions) of the electrocatalysts. The formation of 3D vdW hybrid with graphene regulates the electronic structure of N-MoS_2 and renders the TMD nanosheets more exposed to the electrolyte. Significantly reduced R_{ct} can also be observed on the 3D vdW hybrids by A.C. impedance tests. Moreover, G@N-MoS_2 also exhibits superior HER, ORR, and OER activity in 0.10 M KOH electrolyte. The construction of 3D vdW hybrid of graphene and N-MoS_2 is one of the critical reasons for the high electrocatalytic activity.

In HER electrocatalysis, the adsorption energy of hydrogen atoms on the active sites should be optimized to zero to achieve the best activity [47]. The HER mechanism on MoS_2/graphene vdW heterostructure was investigated using density functional theory (DFT) calculations by Narayanan et al. [48]. The charge transfer

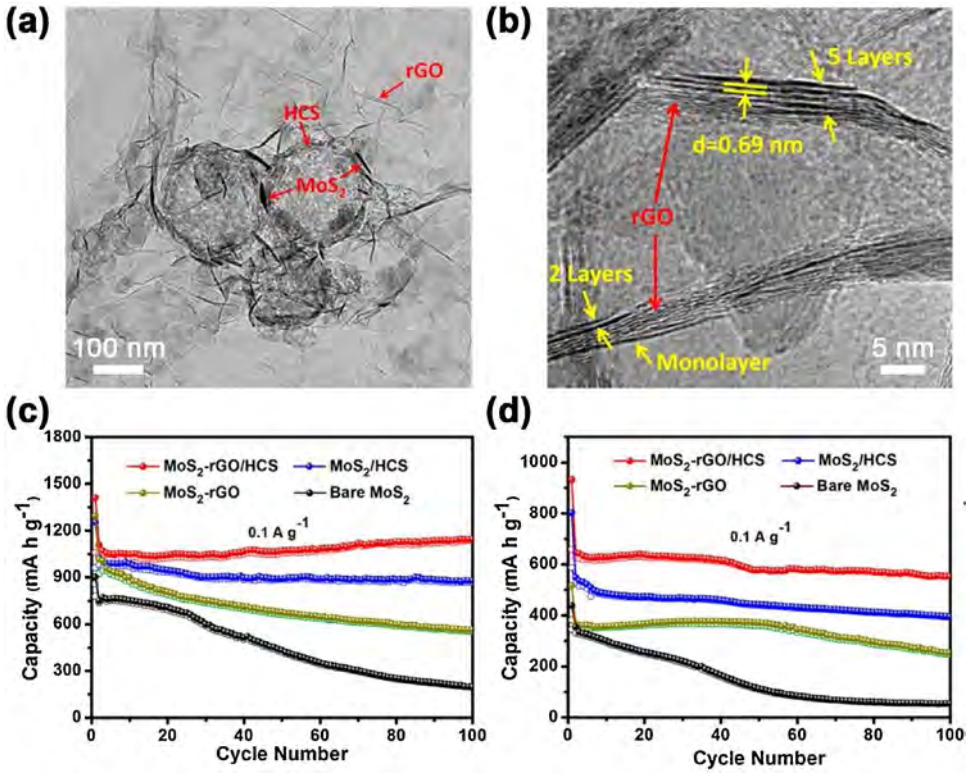

Fig. 3. The hybrid of MoS_2 and rGO for Li and Na storage. (a) TEM and (b) HRTEM images of MoS_2-rGO/HCS. (c) Lithium ion battery and (d) sodium ion battery cycling performances of the hybrid material.

Reproduced with permission from Ref. [52]. Copyright 2018, American Chemical Society.

from graphene to MoS_2 in the vdW hybrid renders the hydrogen adsorption energy on the graphene side closer to zero. Therefore, in 3D vdW hybrids of molybdenum/tungsten dichalcogenides and 3D graphene, the vdW interaction between two materials improves the intrinsic activity, and the 3D graphene framework makes the dichalcogenides more uniformly dispersed and more exposed to the reactants. Consequently, the 3D vdW hybrids can achieve high performances in energy electrocatalysis.

The 3D vdW hybrids of TMD and graphene were not only investigated for the use in electrocatalysis, but also in other applications such as metal ion batteries, supercapacitors, etc. [49–51]. The Li and Na storage properties of few-layer MoS_2 nanosheets supported by reduced GO (rGO) cross-linked hollow carbon spheres (HCS) was reported by Wen et al. [52]. The MoS_2 nanosheets were *in-situ* grown on the surface of rGO and HCS, forming a 3D vdW hybrid. The morphology of MoS_2-rGO/HCS is shown in Fig. 3a and 3b. The cross-linked structure of rGO and HCS, and the MoS_2 nanosheets grown on them can be observed in TEM image in Fig. 3a. The HRTEM image (Fig. 3b) confirmed the structure of few-layer MoS_2 stacking on graphene. The interlayer distance of MoS_2 is 0.69 nm, larger than the lattice spacing of (002) crystal planes. The enlarged interlayer distance benefits the reversible intercalation/deintercalation of Li and Na ions in the metal ion batteries. Then the MoS_2-rGO/HCS hybrid was employed in Li-ion batteries (Fig. 3c) and Na ion batteries (Fig. 3d), exhibiting a reversible capacity of 1145 and 552 mAh g^{-1} at 0.1 A g^{-1} after 100 cycles for Li and Na ion batteries, respectively. The formation of 3D vdW hybrids of MoS_2 nanosheets and 3D graphene networks avoids the agglomeration of MoS_2, realizing efficient connection of MoS_2 and graphene to enhance the electrical conductivity. Together with the enlarged interlayer distance of MoS_2, the metal ion battery performances were significantly enhanced in this 3D vdW hybrid.

3D vdW hybrids of other transition metal compounds and graphene

Metal compounds beyond dichalcogenides also contribute as an important part of the 2D material family [17]. Metal oxides [53,54], hydroxides [13], nitrides and carbides (MXenes) [55,56], and other types of metal compounds with 2D crystal structure [57–59] have exhibited their significant roles on energy-related applications. Herein, research progresses on the 3D hybrids of these metal compound 2D materials and graphene are reviewed.

The widely investigated 2D metal oxide materials in energy chemistry field include TiO_2, V_2O_5, MnO_2, WO_3, perovskite-like crystals, etc. [53,60,61]. The design and synthesis of the 3D vdW hybrids of metal oxides and graphene were also strongly considered. Recently, Feng and Wu et al. [62] synthesized freestanding V_2O_5/graphene films by taking the advantage of the self-assembly of V_2O_5 nanobelts and GO nanosheets in their mixed liquid-crystal phase suspension. After vacuum filtration of the suspension, flexible V_2O_5/graphene composite films with highly oriented layered structures were obtained (Fig. 4a). In the films, both V_2O_5 nanobelts and GO are stacked together by vdW interaction, obtaining a macroscopic 3D hybrid. The scanning electronic microscopy (SEM) image (Fig. 4b) of the hybrid confirms the layered structure. The elemental mapping verifies the uniform dispersion of V_2O_5 and graphene in the composite. The freestanding V_2O_5/graphene hybrid films then exhibited good performance in flexible supercapacitors. The composites of graphene and various kinds of 2D metal oxides, including V_2O_5 and MnO_2, have been demonstrated impressive performance in supercapacitors [63–65].

The 2D metal oxide/graphene hybrids can be employed in many types of energy storage devices, such as serving as the cathode materials for metal-ion batteries [66–73] to improve ion storage

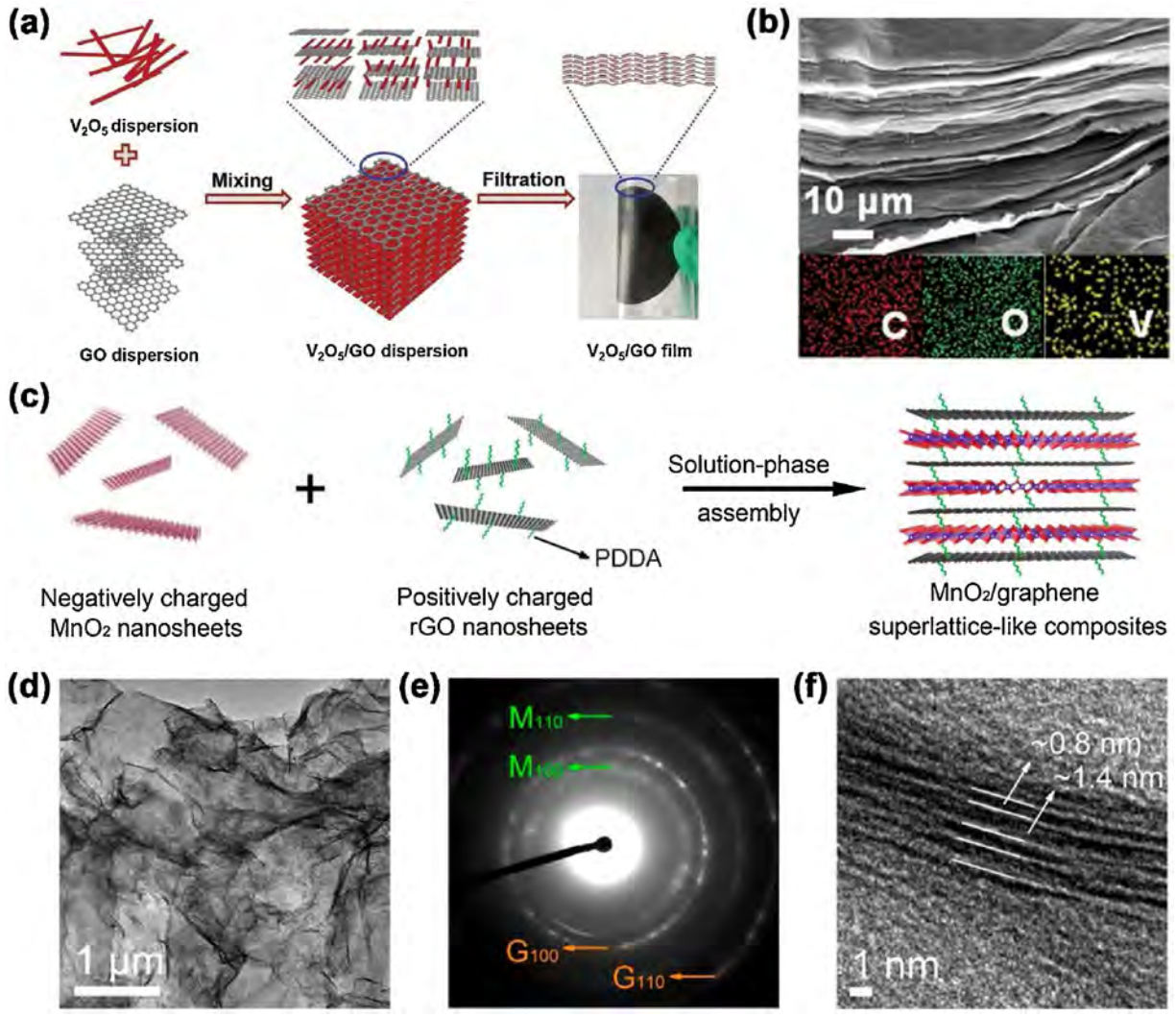

Fig. 4. Hybrids of 2D oxides and graphene materials. (a) The illustration for the synthesis process of V_2O_5/graphene composite films. (b) SEM image and elemental mapping profile of V_2O_5/graphene composite. Reproduced with permission from Ref. [62]. Copyright 2017, Wiley-VCH. (c) The assembly process of MnO_2/graphene superlattice-like composite. (d) TEM image, (e) selected area electron diff ;raction pattern, and (f) HRTEM image of MnO_2/graphene composite.
Reproduced with permission from Ref. [76]. Copyright 2018, American Chemical Society.

performance, and for lithium–sulfur batteries [74] to boost the sulfur utilization efficiency, etc. For example, MoO_3/graphene composites have been widely investigated in lithium-ion batteries for their high lithium ion storage properties [67–71]. Recently, Cui et al. [75] conducted first-principle studies on MoO_3/graphene composites, and verified that the vdW-connected MoO_3/graphene hybrids could afford extremely lower Li diffusion barrier than bulk MoO_3 material, thus leading to fast Li charge/discharge rates.

The hybridization of MnO_2 and graphene monolayers for superior Li and Na storage was also reported by Sasaki et al. [76]. As illustrated in Fig. 4c, negatively charged single-layer MnO_2 nanosheets and poly-(diallyldimethylammonium chloride) (PDDA) modified positively charged single-layer rGO nanosheets were mixed up in solution phase to fabricate a superlattice-like composite. The ratio of MnO_2 and rGO was calculated to achieve layer-by-layer stacking. Fig. 4d illustrates the transmission electron microscopy (TEM) image of the MnO_2/graphene hybrid. A 3D microstructure can be observed. The selected area electron diff ;raction (SAED) pattern (Fig. 4e) reveals the diffraction rings of both MnO_2 and graphene, confirming the co-existence and intimate coupling of MnO_2 and graphene nanosheets. Moreover, the HRTEM image (Fig. 4f) clearly shows alternating lattice fringes corresponding to MnO_2 and rGO, respectively, indicating the formation of a vdW hybrid. The as-obtained MnO_2/graphene hybrid material then exhibited excellent Li/Na storage performance in Li and Na ion batteries, with the specific capacity of 1325 and 795 mA h g^{-1} at 0.1 A g^{-1} for Li and Na storage, respectively. The superior performances can be attributed to the unique unilamellar vdW hybridization of MnO_2 and rGO. The single-layer MnO_2 shortened the ion diffusion pathway, and the graphene layers in the hybrid improved the electrical conductivity, leading to fast charge transport.

2D transition metal hydroxides, such as brucites and their derivatives, are also frequently used in various energy applications [77]. LDHs are brucite-like hydroxides with two or more kinds of metal ions in the lattice [78]. In applications like electrocatalysis, the synergistic effect of the metal ions in LDHs can boost their performance [79,80]. Fig. 5 affords an example of the hybridization of nanosized NiFe LDH and nitrogen-doped graphene framework (NGF) to form a 3D vdW composite, and its use in OER electrocatalysis [81]. The nNiFe LDH/NGF hybrid was prepared by depositing LDH nanosheets on NGF in solution phase. NGF affords a porous morphology with abundant mesopores. The nitrogen heteroatoms served as the nucleation centers of LDHs in the synthesis process, and the growth of LDH nanosheets was confined in the meso-

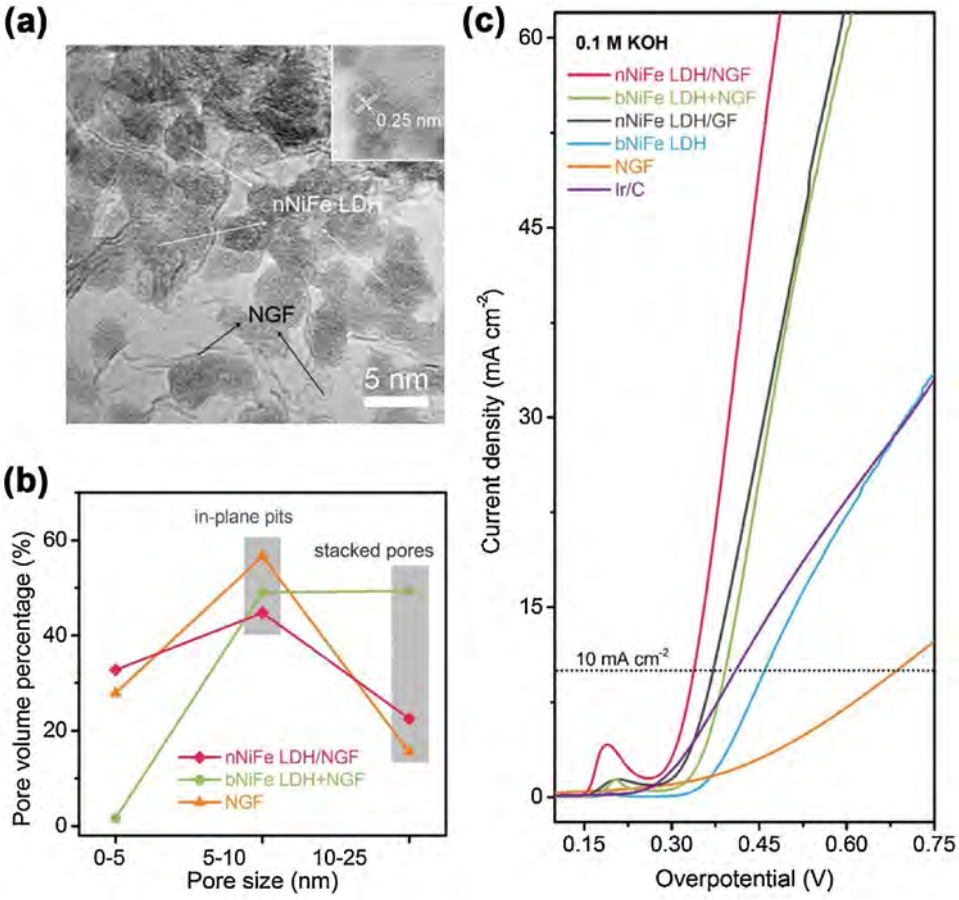

Fig. 5. LDH/graphene composite for OER electrocatalysis. (a) TEM image of nNiFe LDH/NGF. (b) Pore distribution of LDH/graphene composite and contrast samples. (c) OER LSV plots tested in 0.10 M KOH electrolyte.

Reproduced with permission from Ref. [81]. Copyright 2015, Wiley-VCH.

pores, resulting in a small size of less than 10 nm (Fig. 5a). The pore distributions of nNiFe LDH/NGF and NGF wer analyzed by N_2 adsorption/desorption experiments, and the mixture of bulk NiFe LDH and NGF (bNiFe LDH + NGF) was also tested as a contrast sample (Fig. 5b). The results revealed that nNiFe LDH/NGF basically retained the morphology of NGF, while stacked pores large than 10 nm dramatically increased in bNiFe LDH + NGF. It can be indicated that the LDH nanosheets were adhered on the graphene framework face-to-face in nNiFe LDH/NGF, forming a 3D vdW hybrid. In OER electrocatalysis, the 3D hybrid material exhibited a small overpotential of 337 mV for 10 mA cm^{-2} current density in 0.10 M KOH electrolyte (Fig. 5c). The small particle size of NiFe LDHs resulting from their hybridization with graphene is a critical reason for the high OER activity.

MXenes, a family of 2D transition metal carbides and nitrides with metallic conductivity and high hydrophilicity, are attracting increasing attention in supercapacitors, metal ion batteries, etc. [55,56]. Recently, a 3D MXene-graphene composite was proposed by Gao and co-workers for the application in supercapacitors [82]. As illustrated by Fig. 6a, the mixed solution of MXene and graphene was freeze-dried and reduced to prepare 3D MXene-rGO aerogel. After freeze-drying, the graphene sheets constructed a 3D framework, and formed composites with MXene. The SEM image in Fig. 6b exhibits the 3D porous structure of MXene-rGO composite. The coexistence of MXene and graphene in the composite was confirmed by XRD spectra (Fig. 6c). Then the 3D MXene-rGO composite exhibited an area capacitance of 34.6 m F cm^{-2} at a scan rate of 1 mV s^{-1} (Fig. 6d), and high stability after 15,000 cycles at 2 mA cm^{-2} (Fig. 6e) in the electrochemical tests. More innovative researches on the combination of emerging MXene materials and graphene are expected in the future.

3D vdW hybrids of metal-free 2D materials and graphene

2D metal-free graphene analogues, including graphitic carbon nitride (g-C_3N_4) [83–85], hexagonal boron nitride (hBN) [86], etc. [87,88], have proven their significance in the fields of semiconductor [89,90], electrochemical energy storage [91,92], and so on. By the hybridization with graphene materials, the conductivity of these 2D materials can be improved, and the morphology can also be regulated. The g-C_3N_4 material can be regarded as a 2D carbon nanomaterial with high nitrogen doping ratio and abundant defects, showing great potential in photocatalytic and electrocatalytic hydrogen production, oxygen electrocatalysis, etc. Owing to the poor electrical conductivity of g-C_3N_4, g-C_3N_4/graphene composites have been widely investigated to enhance the conductivity and the performance in electrochemical applications [92–95]. The face-to-face stacking of few-layer g-C_3N_4 and graphene with a 3D vdW heterostructure was also explored [96–98].

Recently, Yan et al. reported a composite of graphene and ultrathin C_3N_4 quantum dots for HER electrocatalysis [96]. The C_3N_4 quantum dots (CNQDs) were prepared by the ultrasound-assisted exfoliation of bulk g-C_3N_4. Then the composite material was obtained via hydrothermal hybridization of CNQDs and GO. Fig. 7a provides the atomic force microscopy (AFM) of the CNQDs@G hybrid material. CNQDs with a thickness of 0.4 nm and graphene with a thickness of 1 nm were intimately contacted. The TEM image (Fig. 7b) reveals the uniform distribution of CNQDs on graphene.

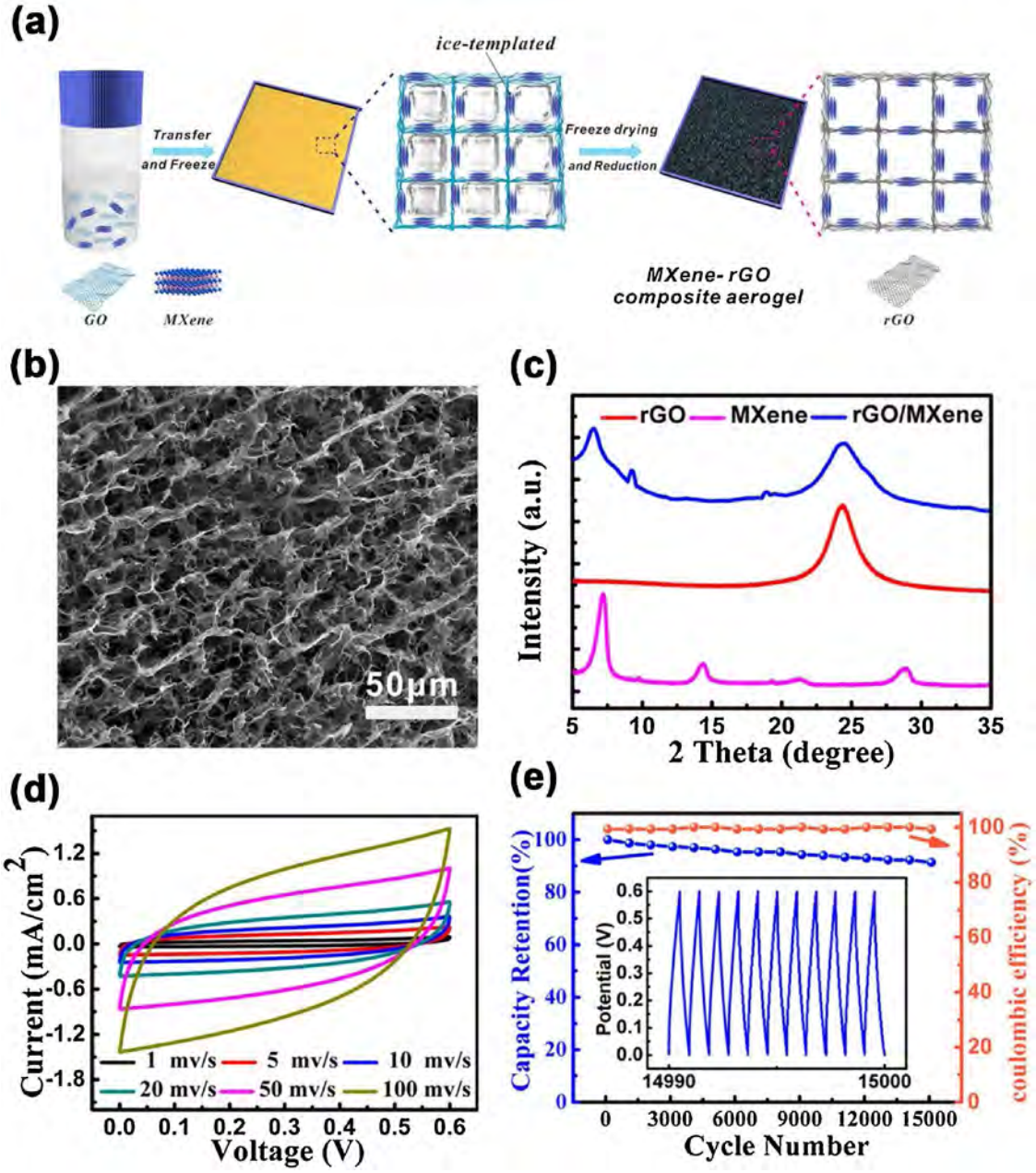

Fig. 6. MXene/rGO composite for supercapacitors. (a) Schematic illustration for the synthesis of MXene-rGO composite aerogel. (b) SEM image of rGO/MXene. (c) XRD patterns of rGO, MXene and rGO/MXene. (d) Cyclic voltammogram (CV) curves of MXene/rGO composite at different scan rates. (e) Cycling stability of MXene/rGO composite at the current density of 2 mA cm^{-2}.

Reproduced with permission from Ref. [82]. Copyright 2018, American Chemical Society.

The HER activity of such a C_3N_4/graphene vdW heterostructure was analyzed by first-principle calculation. Fig. 7c exhibits the molecular model and the interface charge transfer of CNQDs@G. The charge distribution on the edges of CNQDs indicates the edges to be potential active sites. The free energy diagrams of HER process on the catalysts (Fig. 7d) reveals that the Gibbs free energy of the intermediate state (ΔG_{H^*}) on CNQDs@G is near zero, similar to that of Pt electrocatalyst. Thus, excellent HER activity of CNQDs@G can be expected from the above first-principle analysis.

The HER performance of CNQDs@G was tested in 0.5 M H_2SO_4 electrolyte. The overpotential for 10 mA cm^{-2} current density is only 110 mV for CNQDs@G, as shown by the LSV plots (Fig. 7e). The stability and Faradaic efficiency were also characterized (Fig. 7f). The HER current density showed no obvious change after 10 h at a constant overpotential of 110 mV. The Faradaic efficiency was calculated by comparing the theoretical H_2 yield and the amount of H_2 collected in the electrocatalysis process, which is almost 100%. From both theoretical and experimental analyses, the vdW hybrid of C_3N_4 quantum dots and graphene was verified as a highly active HER electrocatalyst.

For other metal-free 2D materials, their vdW hybrids with graphene for energy applications still need to be explored. For instance, hBN is a highly stable 2D material, and has shown excellent performances in electronic, dielectric, and optical applications [99]. The vdW heterostructure of hBN and graphene also shows the potential for the application in solar cells [100,101]. More efforts are expected to be made on the 3D vdW hybrid of graphene and other 2D metal-free materials, to explore their applications in energy-related fields.

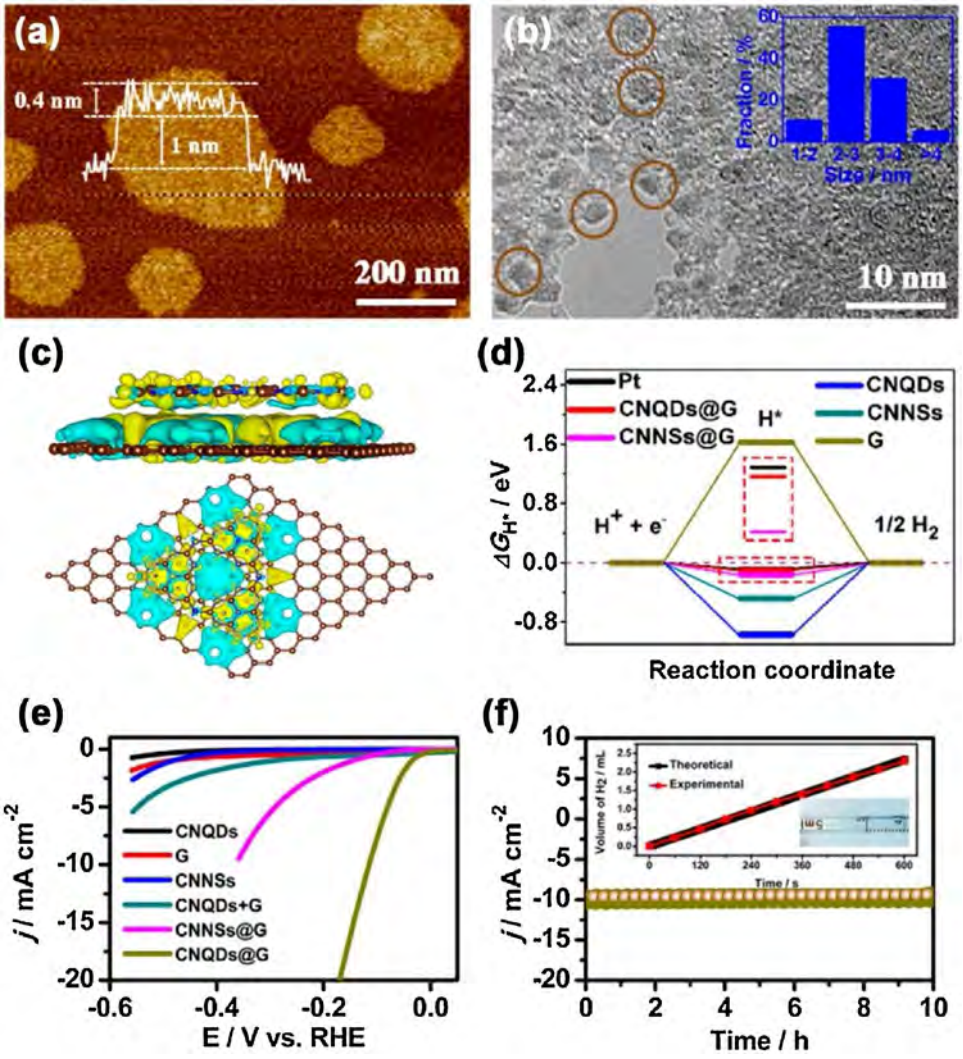

Fig. 7. The hybrid of C_3N_4 quantum dots and graphene for HER electrocatalysis. (a) AFM images of CNQDs@G hybrid. Inset: the corresponding height curve. (b) TEM image of CNQDs@G hybrid. Inset: size distribution. (c) Schematic structure and interfacial transfer of CNQDs@G. (d) Free energy diagrams for HER. (e) HER performances evaluated in 0.5 M H_2SO_4 electrolyte. (f) HER stability test of CNQDs@G at the overpotential of 110 mV. Inset: theoretical and experimental H_2 yield.
Reproduced with permission from Ref. [96]. Copyright 2018, American Chemical Society.

3D vdW hybrids of multiple 2D materials and graphene

Besides using a single 2D material to fabricate 3D vdW hybrids with graphene, the hybrids of graphene and more than one kinds of 2D materials can further extend the types of their applications. The reported combinations of the 2D materials include graphene/g-C_3N_4/MoS_2 [102–105], graphene/g-C_3N_4/$Ni(OH)_2$ [106], etc. However, most of the reported works on the hybridization of multiple 2D materials and graphene did not aim at fabricating vdW hybrids. The direct evidence for the LEGO-like stacking of all components is hard to be found. For example, a g-C_3N_4/graphene/MoS_2 hybrid material for photocatalytic H_2 production was recently reported [102]. As illustrated by Fig. 8a, g-C_3N_4 was firstly combined with graphene by the pyrolysis of GO/urea composite, and GO was reduced to rGO in this process. Then MoS_2 was deposited on g-C_3N_4/rGO through a hydrothermal treatment to obtain g-C_3N_4/graphene/MoS_2. The TEM and HRTEM images of this hybrid material are presented in Fig. 8b-d. The hybrid material affords a 3D porous structure, but most of the MoS_2 nanosheets were grown on graphene, without interactions with g-C_3N_4. Although g-C_3N_4 is also a 2D material in this hybrid, the vdW heterostructures mainly fabricated by the layers of graphene and MoS_2. The fabrication of 3D van der Waals heterostructures of multiple 2D materials is promising for the well integration of the 2D materials, which is worth to be explored in the future.

Summary and outlook

Fabricating graphene-based 3D vdW hybrids is an emerging and effective strategy for the design of 2D-material-based energy materials. The combination of 2D nanomaterials and 3D graphene framework can take the advantages of the features of 3D graphene, including high electrical conductivity, porous structure, and high specific surface area. Through the rational integration of 2D materials and 3D graphene, the 2D materials can be transformed into 3D nanostructure, thus bringing more possibilities for the structural design and property demonstration of 2D materials. As an emerging topic in the fields of energy materials, 3D vdW hybrids for energy applications are still not well investigated. Some perspectives for the future investigation on 3D vdW hybrids are presented as follows:

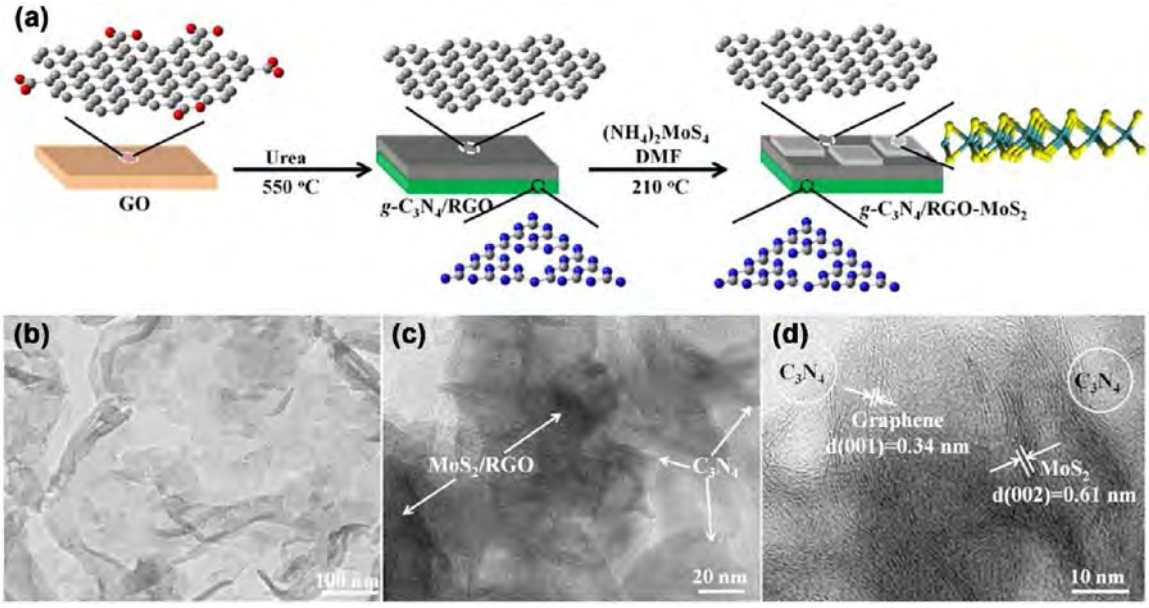

Fig. 8. A three-component composite of graphene, g-C_3N_4 and MoS_2. (a) Schematic illustration for the synthesis process. (b–c) TEM images and (d) HRTEM image of g-C_3N_4/graphene/MoS_2.
Reproduced with permission from Ref. [102]. Copyright 2018, American Chemical Society.

(1) The fabrication of 3D vdW hybrids from 2D materials brings about a new category of materials, with the unique features of curving surface, asymmetric structure, abundant interfaces, size effect, etc. New methods need to be established to gain deeper understandings on the features of 3D vdW hybrids, thus benefiting the structural regulation of 2D materials.
(2) Efforts need to be made to clearly identify the vdW hybridization as the origin of the property changes and the performance improvements in 2D material composites.
(3) The interconnected frameworks for electron transfer and porous channels for ion transfer in graphene-based 3D vdW hybrids provide great opportunities in electrochemical energy storage. The precision synthesis of 3D vdW hybrids to meet the requirements of capacitors, batteries or optoelectronic devices is also worth studying.
(4) The practical application of 3D vdW hybrids requires the mass production of them. Green, efficient and economic technologies need to be developed.
(5) Emerging applications for graphene-based 3D vdW hybrids are strongly considered. 3D graphene-based materials and composites have been investigated for the surface modification of Li metal anodes [107–110]. The rational design of graphene-based 3D vdW hybrids is highly expected for safe Li metal batteries.
(6) 2D materials beyond graphene also have the potential to serve as the 3D host to generate vdW heterostructures, bringing about more novel properties of the 3D vdW hybrids. For example, the 3D MXenes [111] and 3D g-C_3N_4 [112,113] that have been reported and applied in energy fields.

The transformation from 2D to 3D benefits the practical application of 2D materials and offers new promising candidates for various fields. Based on the fundamental understandings on 2D materials, and the construction strategies of 3D materials, the advantages of 2D materials can be highlighted on 3D vdW heterostructures. The exploration of micro- and nano-scale materials is a cutting-edge topic, which requires the combination of the methodologies in material, physics, chemistry, and engineering. It's expected that this review can inspire more insights on 3D graphene and 3D vdW hybrids, to further boost the researches on materials for energy conversion and storage.

Acknowledgements

This work was supported by National Key Research and Development Program (2016YFA0202500 and 2016YFA0200101) and National Natural Scientific Foundation of China (21676160 and 21825501), and Tsinghua University Initiative Scientific Research Program. We thank Bo-Quan Li and Bin Wang for helpful discussion.

Appendix A. Supplementary data

Supplementary material related to this article can be found, in the online version, at doi:https://doi.org/10.1016/j.nantod.2019.02.006.

References

[1] K.S. Novoselov, A.K. Geim, S.V. Morozov, D. Jiang, Y. Zhang, S.V. Dubonos, I.V. Grigorieva, A.A. Firsov, Science 306 (2004) 666–669.
[2] H.Y. Jin, C.X. Guo, X. Liu, J.L. Liu, A. Vasileff, Y. Jiao, Y. Zheng, S.Z. Qiao, Chem. Rev. 118 (2018) 6337–6408.
[3] W. Zhang, K. Zhou,Small 13 (2017), 1700806.
[4] Y. Wang, Z.Q. Shi, Y. Huang, Y.F. Ma, C.Y. Wang, M.M. Chen, Y.S. Chen, J. Phys. Chem. C 113 (2009) 13103–13107.
[5] Y. Huang, J.J. Liang, Y.S. Chen, Small 8 (2012) 1805–1834.
[6] Y. Han, Y. Ge, Y.F. Chao, C.Y. Wang, G.G. Wallace, J. Energy Chem. 27 (2018) 57–72.
[7] Y. Xie, M. Naguib, V.N. Mochalin, M.W. Barsoum, Y. Gogotsi, X.Q. Yu, K.W. Nam, X.Q. Yang, A.I. Kolesnikov, P.R.C. Kent, J. Am. Chem. Soc. 136 (2014) 6385–6394.
[8] K. Yan, H.W. Lee, T. Gao, G.Y. Zheng, H.B. Yao, H.T. Wang, Z.D. Lu, Y. Zhou, Z. Liang, Z.F. Liu, S. Chu, Y. Cui, Nano Lett. 14 (2014) 6016–6022.
[9] N. Jiang, B. Li, F.H. Ning, D.G. Xia, J. Energy Chem. 27 (2018) 1651–1654.
[10] D. Zhang, S. Wang, Y. Ma, S.B. Yang, J. Energy Chem. 27 (2018) 128–145.
[11] H.T. Yuan, H.T. Wang, Y. Cui, Acc. Chem. Res. 48 (2015) 81–90.
[12] C.L. Tan, X.H. Cao, X.J. Wu, Q.Y. He, J. Yang, X. Zhang, J.Z. Chen, W. Zhao, S.K. Han, G.H. Nam, M. Sindoro, H. Zhang, Chem. Rev. 117 (2017) 6225–6331.
[13] H.J. Yin, Z.Y. Tang, Chem. Soc. Rev. 45 (2016) 4873–4891.
[14] H.C. Tao, Y.A. Gao, N. Talreja, F. Guo, J. Texter, C. Yan, Z.Y. Sun, J. Mater. Chem. A 5 (2017) 7257–7284.
[15] W.L. Yang, X.D. Zhang, Y. Xie, Nano Today 11 (2016) 793–816.
[16] H. Wang, H.B. Feng, J.H. Li, Small 10 (2014) 2165–2181.
[17] A.K. Geim, I.V. Grigorieva, Nature 499 (2013) 419–425.

[18] D. Jariwala, T.J. Marks, M.C. Hersam, Nat. Mater. 16 (2017) 170–181.
[19] J.J. Linghu, T. Yang, Y.Z. Luo, M. Yang, J. Zhou, L. Shen, Y.P. Feng, ACS Appl. Mater. Interfaces 10 (2018) 32142–32150.
[20] H. Xu, J.J. Yi, X.J. She, Q. Liu, L. Song, S.M. Chen, Y.C. Yang, Y.H. Song, R. Vajtai, J. Lou, H.M. Li, S.Q. Yuan, J.J. Wu, P.M. Ajayan, Appl. Catal. B 220 (2018) 379–385.
[21] H.U. Din, M. Idrees, G. Rehman, C.V. Nguyen, L.Y. Gan, I. Ahmad, M. Maqbool, B. Amin, Phys. Chem. Chem. Phys. 20 (2018) 24168–24175.
[22] C.L. Li, Q. Cao, F.Z. Wang, Y.Q. Xiao, Y.B. Li, J.J. Delaunay, H.W. Zhu, Chem. Soc. Rev. 47 (2018) 4981–5037.
[23] W.S. Xia, L.P. Dai, P. Yu, X. Tong, W.P. Song, G.J. Zhang, Z.M. Wang, Nanoscale 9 (2017) 4324–4365.
[24] A.A. Balandin, S. Ghosh, W.Z. Bao, I. Calizo, D. Teweldebrhan, F. Miao, C.N. Lau, Nano Lett. 8 (2008) 902–907.
[25] A.H. Castro Neto, F. Guinea, N.M.R. Peres, K.S. Novoselov, A.K. Geim, Rev. Mod. Phys. 81 (2009) 109–162.
[26] C. Lee, X.D. Wei, J.W. Kysar, J. Hone, Science 321 (2008) 385–388.
[27] C. Tang, M.M. Titirici, Q. Zhang, J. Energy Chem. 26 (2017) 1077–1093.
[28] K.S. Novoselov, V.I. Fal'ko, L. Colombo, P.R. Gellert, M.G. Schwab, K. Kim, Nature 490 (2012) 192–200.
[29] Y.X. Xu, G.Q. Shi, X.F. Duan, Acc. Chem. Res. 48 (2015) 1666–1675.
[30] F.X. Bu, I. Shakir, Y.X. Xu,Adv. Mater. Interfaces 5 (2018), 1800468.
[31] K. Chen, L.R. Shi, Y.F. Zhang, Z.F. Liu, Chem. Soc. Rev. 47 (2018) 3018–3036.
[32] X.H. Cao, Z.Y. Yin, H. Zhang, Energy Environ. Sci. 7 (2014) 1850–1865.
[33] Y. Xu, C. Cheng, S.C. Du, J.Y. Yang, B. Yu, J. Luo, W.Y. Yin, E.P. Li, S.R. Dong, P.D. Ye, X.F. Duan, ACS Nano 10 (2016) 4895–4919.
[34] X. Huang, Z.Y. Zeng, H. Zhang, Chem. Soc. Rev. 42 (2013) 1934–1946.
[35] D. Jariwala, V.K. Sangwan, L.J. Lauhon, T.J. Marks, M.C. Hersam, ACS Nano 8 (2014) 1102–1120.
[36] Y. Yan, B.Y. Xia, Z.C. Xu, X. Wang, ACS Catal. 4 (2014) 1693–1705.
[37] X.H. Cao, C.L. Tan, X. Zhang, W. Zhao, H. Zhang, Adv. Mater. 28 (2016) 6167–6196.
[38] X. Li, J.Y. Shan, W.Z. Zhang, S. Su, L.H. Yuwen, L.H. Wang,Small 13 (2017), 1602660.
[39] K. Chang, X. Hai, J.H. Ye,Adv. Energy Mater. 6 (2016), 1502555.
[40] X.Y. Chia, M. Pumera, Chem. Soc. Rev. 47 (2018) 5602–5613.
[41] M. Zeng, Y.G. Li, J. Mater. Chem. A 3 (2015) 14942–14962.
[42] Q.P. Lu, Y.F. Yu, Q.L. Ma, B. Chen, H. Zhang, Adv. Mater. 28 (2016) 1917–1933.
[43] L. Liao, J. Zhu, X.J. Bian, L.N. Zhu, M.D. Scanlon, H.H. Girault, B.H. Liu, Adv. Funct. Mater. 23 (2013) 5326–5333.
[44] J.J. Duan, S. Chen, B.A. Chambers, G.G. Andersson, S.Z. Qiao, Adv. Mater. 27 (2015) 4234–4241.
[45] S.J. Xu, Z.Y. Lei, P.Y. Wu, J. Mater. Chem. A 3 (2015) 16337–16347.
[46] C. Tang, L. Zhong, B.S. Zhang, H.F. Wang, Q. Zhang,Adv. Mater. 30 (2018), 1705110.
[47] T. Ling, D.Y. Yan, H. Wang, Y. Jiao, Z.P. Hu, Y. Zheng, L.R. Zheng, J. Mao, H. Liu, X.W. Du, M. Jaroniec, S.Z. Qiao, Nat. Commun. 8 (2017) 1509.
[48] R.K. Biroju, D. Das, R. Sharma, S. Pal, L.P.L. Mawlong, K. Bhorkar, P.K. Giri, A.K. Singh, T.N. Narayanan, ACS Energy Lett. 2 (2017) 1355–1361.
[49] L.F. Jiang, B.H. Lin, X.M. Li, X.F. Song, H. Xia, L. Li, H.B. Zeng, ACS Appl. Mater. Interfaces 8 (2016) 2680–2687.
[50] Z.N. Deng, H. Jiang, C.Z. Li,Small 14 (2018), 1800148.
[51] Q.Q. Yang, M.C. Liu, Y.M. Hu, Y. Xu, L.B. Kong, L. Kang, J. Energy Chem. 27 (2018) 1208–1213.
[52] X. Hu, Y. Li, G. Zeng, J.C. Jia, H.B. Zhan, Z.H. Wen, ACS Nano 12 (2018) 1592–1602.
[53] J. Mei, T. Liao, L.Z. Kou, Z.Q. Sun,Adv. Mater. 29 (2017), 1700176.
[54] J. Mei, T. Liao, Z.Q. Sun, J. Energy Chem. 27 (2018) 117–127.
[55] X. Zhang, Z.H. Zhang, Z. Zhou, J. Energy Chem. 27 (2018) 73–85.
[56] V.M.H. Ng, H. Huang, K. Zhou, P.S. Lee, W.X. Que, J.Z. Xu, L.B. Kong, J. Mater. Chem. A 5 (2017) 3039–3068.
[57] R. Xu, Y.Z. Sun, Y.F. Wang, J.Q. Huang, Q. Zhang, Chin. Chem. Lett. 28 (2017) 2235–2238.
[58] C. Zeng, F.X. Xie, X.F. Yang, M. Jaroniec, L. Zhang, S.Z. Qiao, Angew. Chem. Int. Ed. 57 (2018) 8540–8544.
[59] J.L. Liu, D.D. Zhu, Y. Zheng, A. Vasileff, S.Z. Qiao, ACS Catal. 8 (2018) 6707–6732.
[60] M. Osada, T. Sasaki, Dalton Trans. 47 (2018) 2841–2851.
[61] R.Z. Ma, T. Sasaki, Accounts. Chem. Res. 48 (2015) 136–143.
[62] H.Q. Liu, Y.P. Tang, C. Wang, Z.X. Xu, C.Q. Yang, T. Huang, F. Zhang, D.Q. Wu, X.L. Feng,Adv. Funct. Mater. 27 (2017), 1606269.
[63] A.K. Mondal, B. Wang, D.W. Su, Y. Wang, S.Q. Chen, X.G. Zhang, G.X. Wang, Mater. Chem. Phys. 143 (2014) 740–746.
[64] L.L. Peng, X. Peng, B.R. Liu, C.Z. Wu, Y. Xie, G.H. Yu, Nano Lett. 13 (2013) 2151–2157.
[65] G. Yilmaz, X.M. Lu, G.W. Ho, Nanoscale 9 (2017) 802–811.
[66] H.C. Tao, L.Z. Fan, X.Q. Yan, X.H. Qu, Electrochim. Acta 69 (2012) 328–333.
[67] Q. Xia, H.L. Zhao, Z.H. Du, Z.P. Zeng, C.H. Gao, Z.J. Zhang, X.F. Du, A. Kulka, K. Swierczek, Electrochim. Acta 180 (2015) 947–956.
[68] C.L. Liu, Y. Wang, C. Zhang, X.S. Li, W.S. Dong, Mater. Chem. Phys. 143 (2014) 1111–1118.
[69] P.B. Wang, Z.H. Cheng, G.Q. Lv, L.T. Qu, Y. Zhao, Nanoscale 10 (2018) 396–402.
[70] P.J. Lu, M. Lei, J. Liu, CrystEngComm 16 (2014) 6745–6755.
[71] L. Noerochim, J.Z. Wang, D. Wexler, Z. Chao, H.K. Liu, J. Power Sources 228 (2013) 198–205.
[72] B.S. Li, B.J. Xi, Z.Y. Feng, Y. Lin, J.C. Liu, J.K. Feng, Y.T. Qian, S.L. Xiong,Adv. Mater. 30 (2018), 1705788.
[73] G.L. Xu, L.S. Xiao, T. Sheng, J.Z. Liu, Y.X. Hu, T.Y. Ma, R. Amine, Y.Y. Xie, X.Y. Zhang, Y.Z. Liu, Y. Ren, C.J. Sun, S.M. Heald, J. Kovacevic, Y.H. Sehlleier, C. Schulz, W.L. Mattis, S.G. Sun, H. Wiggers, Z.H. Chen, K. Amine, Nano Lett. 18 (2018) 336–346.
[74] M.P. Yu, J.S. Ma, H.Q. Song, A.J. Wang, F.Y. Tian, Y.S. Wang, H. Qiu, R.M. Wang, Energy Environ. Sci. 9 (2016) 1495–1503.
[75] Y.H. Cui, Y. Zhao, H. Chen, K.Y. Wei, S. Ni, Y.X. Cui, S.Q. Shi, Appl. Surf. Sci. 433 (2018) 1083–1093.
[76] P. Xiong, R.Z. Ma, N. Sakai, T. Sasaki, ACS Nano 12 (2018) 1768–1777.
[77] R.Z. Ma, T. Sasaki, Adv. Mater. 22 (2010) 5082–5104.
[78] G.L. Fan, F. Li, D.G. Evans, X. Duan, Chem. Soc. Rev. 43 (2014) 7040–7066.
[79] C. Tang, H.F. Wang, H.S. Wang, F. Wei, Q. Zhang, J. Mater. Chem. A 4 (2016) 3210–3216.
[80] C. Tang, H.F. Wang, X.L. Zhu, B.Q. Li, Q. Zhang, Part. Part. Syst. Charact. 33 (2016) 473–486.
[81] C. Tang, H.S. Wang, H.F. Wang, Q. Zhang, G.L. Tian, J.Q. Nie, F. Wei, Adv. Mater. 27 (2015) 4516–4522.
[82] Y. Yue, N. Liu, Y.A. Ma, S.L. Wang, W.J. Liu, C. Luo, H. Zhang, F. Cheng, J.Y. Rao, X.K. Hu, J. Su, Y.H. Gao, ACS Nano 12 (2018) 4224–4232.
[83] J.J. Zhu, P. Xiao, H.L. Li, S.A.C. Carabineiro, ACS Appl. Mater. Interfaces 6 (2014) 16449–16465.
[84] J. Liu, H.Q. Wang, M. Antonietti, Chem. Soc. Rev. 45 (2016) 2308–2326.
[85] Z.W. Zhao, Y.J. Sun, F. Dong, Nanoscale 7 (2015) 15–37.
[86] J. Yin, J.D. Li, Y. Hang, J. Yu, G.A. Tai, X.M. Li, Z.H. Zhang, W.L. Guo, Small 12 (2016) 2942–2968.
[87] S. Balendhran, S. Walia, H. Nili, S. Sriram, M. Bhaskaran, Small 11 (2015) 640–652.
[88] M.Z. Rahman, C.W. Kwong, K. Davey, S.Z. Qiao, Energy Environ. Sci. 9 (2016) 709–728.
[89] D. Akinwande, N. Petrone, J. Hone, Nat. Commun. 5 (2014) 5678.
[90] P. Niu, L.L. Zhang, G. Liu, H.M. Cheng, Adv. Funct. Mater. 22 (2012) 4763–4770.
[91] Y. Zheng, Y. Jiao, M. Jaroniec, Y.G. Jin, S.Z. Qiao, Small 8 (2012) 3550–3566.
[92] Y. Zheng, Y. Jiao, J. Chen, J. Liu, J. Liang, A. Du, W.M. Zhang, Z.H. Zhu, S.C. Smith, M. Jaroniec, G.Q. Lu, S.Z. Qiao, J. Am. Chem. Soc. 133 (2011) 20116–20119.
[93] S.S. Shinde, C.H. Lee, A. Sami, D.H. Kim, S.U. Lee, J.H. Lee, ACS Nano 11 (2017) 347–357.
[94] T.Y. Ma, S. Dai, M. Jaroniec, S.Z. Qiao, Angew. Chem. Int. Ed. 53 (2014) 7281–7285.
[95] Q. Han, Z.H. Cheng, J. Gao, Y. Zhao, Z.P. Zhang, L.M. Dai, L.T. Qu,Adv. Funct. Mater. 27 (2017), 1606352.
[96] H.X. Zhong, Q. Zhang, J. Wang, X.B. Zhang, X.L. Wei, Z.J. Wu, K. Li, F.L. Meng, D. Bao, J.M. Yan, ACS Catal. 8 (2018) 3965–3970.
[97] J.J. Duan, S. Chen, M. Jaroniec, S.Z. Qiao, ACS Nano 9 (2015) 931–940.
[98] Y. Hou, Z.H. Wen, S.M. Cui, X.L. Feng, J.H. Chen, Nano Lett. 16 (2016) 2268–2277.
[99] K.L. Zhang, Y.L. Feng, F. Wang, Z.C. Yang, J. Wang, J. Mater. Chem. C 5 (2017) 11992–12022.
[100] X.J. Song, J.Y. Sun, Y. Qi, T. Gao, Y.F. Zhang, Z.F. Liu,Adv. Energy Mater. 6 (2016), 1600541.
[101] J.G. Wang, F.C. Ma, M.T. Sun, RSC Adv. 7 (2017) 16801–16822.
[102] Y.-J. Yuan, Y. Yang, Z. Li, D. Chen, S. Wu, G. Fang, W. Bai, M. Ding, L.-X. Yang, D.-P. Cao, Z.-T. Yu, Z.-G. Zou, ACS Appl. Energy Mater. 1 (2018) 1400–1407.
[103] Y. Hou, Z.H. Wen, S.M. Cui, X.R. Guo, J.H. Chen, Adv. Mater. 25 (2013) 6291–6297.
[104] M.H. Wu, L. Li, Y.C. Xue, G. Xu, L. Tang, N. Liu, W.Y. Huang, Appl. Catal. B 228 (2018) 103–112.
[105] Y. Hou, J.Y. Li, Z.H. Wen, S.M. Cui, C. Yuan, J.H. Chen, Nano Energy 8 (2014) 157–164.
[106] L. Li, J. Qin, H.T. Bi, S.L. Gai, F. He, P. Gao, Y.L. Dai, X.T. Zhang, D. Yang, P.P. Yang, Sci. Rep. 7 (2017) 43413.
[107] X.B. Cheng, H.J. Peng, J.Q. Huang, R. Zhang, C.Z. Zhao, Q. Zhang, ACS Nano 9 (2015) 6373–6382.
[108] W. Deng, X.F. Zhou, Q.L. Fang, Z.P. Liu,Adv. Energy Mater. 8 (2018), 1703152.
[109] R. Zhang, X.B. Cheng, C.Z. Zhao, H.J. Peng, J.L. Shi, J.Q. Huang, J.F. Wang, F. Wei, Q. Zhang, Adv. Mater. 28 (2016) 2155–2162.
[110] R. Zhang, X.R. Chen, X. Chen, X.B. Cheng, X.Q. Zhang, C. Yan, Q. Zhang, Angew. Chem. Int. Ed. 56 (2017) 7764–7768.
[111] L.Y. Xiu, Z.Y. Wang, M.Z. Yu, X.H. Wu, J.S. Qiu, ACS Nano 12 (2018) 8017–8028.
[112] Z.F. Chen, S.C. Lu, Q.L. Wu, F. He, N.Q. Zhao, C.N.A. He, C.S. Shi, Nanoscale 10 (2018) 3008–3013.
[113] J. Yan, M.T.F. Rodrigues, Z.L. Song, H.P. Li, H. Xu, H. Liu, J.J. Wu, Y.G. Xu, Y.H. Song, Y. Liu, P. Yu, W. Yang, R. Vajtai, H.M. Li, S.Q. Yuan, P.M. Ajayan,Adv. Funct. Mater. 27 (2017), 1700653.

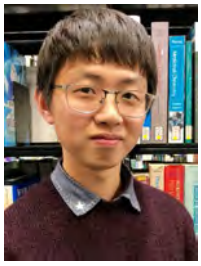

Hao-Fan Wang received his B.S. and Ph.D. degree in 2013 and 2018, respectively, both from the Department of Chemical Engineering, Tsinghua University, under the supervision of Prof. Qiang Zhang. His research focuses on advanced energy materials for the applications on bifunctional oxygen electrocatalysis, metal–air batteries, etc.

Cheng Tang received his Bachelor and Ph.D. degrees from the Department of Chemical Engineering, Tsinghua University in year of 2013 and 2018, respectively. His research interests focus on nanomaterials and energy electrocatalysis, including 3D graphene, hierarchical nanomaterials, oxygen reduction/evolution, hydrogen evolution, nitrogen reduction, etc.

Qiang Zhang received his bachelor and Ph.D. degree from Tsinghua University in 2004 and 2009, respectively. After a stay in Case Western Reserve University, USA, and Fritz Haber Institute of the Max Planck Society, Germany, he was appointed a faculty in Tsinghua University at 2011. His interests focus on energy materials, includes Li-S batteries, Li metal anode, 3D graphene, and electrocatalysts. He has been awarded The National Science Fund for Distinguished Young Scholars, Young Top-Notch Talent from China, and Newton Advanced Fellowship from Royal Society, UK. Currently, he is the associate editor of Journal of Energy Chemistry and sitting on the advisory board of Matter, Advanced Energy Materials, Advanced Materials Interfaces, Philosophical Transactions A, Science China Materials, and so on.